May 15, 2017

Final Report
DOE BES Grant DE-FG02-08ER15929

Computational and Experimental Investigations of the Molecular Scale Structure and Dynamics of Geochemically Important Fluids and Mineral-Fluid Interfaces

Principal Investigator
R. James Kirkpatrick
Departments of Earth and Environmental Sciences and Chemistry
Michigan State University
East Lansing MI, 48824

Co-Principal Investigator
Ozgur Yazaydin
Department of Chemistry
Michigan State University
East Lansing MI, 48824

Contact Information:

Kirkpatrick: e-mail rjkirk@msu.edu, phone 517-353-1132
Yazaydin: e-mail yazaydin@msu.edu, phone 517-355-9715, ext. 336.

I. Introduction

This document serves as the final report for United States Department of Energy Basic Energy Sciences Grant DE-FG02-08ER15929, "*Computational and Spectroscopic Investigations of the Molecular Scale Structure and Dynamics of Geologically Important Fluids and Mineral-Fluid Interfaces*" (R. James Kirkpatrick, P.I., A. O. Yazaydin, co-P.I.). The research under this grant was intimately tied to that supported by the parallel the grant of the same title at Alfred (DOE DE-FG02-10ER16128; Geoffrey M. Bowers, P.I.).

Funding from this grant has resulted in the publication of thirty four peer reviewed scientific papers since its initiation in 2008, with two additional papers already submitted for publication and four in preparation (Table 1). In addition, during this time we have given twenty two invited presentations at scientific meetings, universities and research organizations, and Kirkpatrick has been elected fellow of the American Association for the Advancement of Science, was awarded a Marilyn and Sturges W. Bailey Distinguished Membership in the Clay Minerals Society, and was appointed to a Michigan State University Foundation Professorship.

Table 1: Peer Reviewed Scientific Papers Supported by Grant DE-FG02-08ER15929

1. Kumar P, P., Kalinichev. A.G., and Kirkpatrick, R. J., 2008, Hydrogen-bonding structure and dynamics of aqueous carbonate species from Car-Parrinello molecular dynamics simulations, J. Phys. Chem. B, 113, 794-802.

2. Bowers, G.M., Bish, D.L., and Kirkpatrick, R.J., 2008, H_2O and cation structure and dynamics in expandable clays: ^{2}H and ^{39}K NMR investigations of hectorite, J. Phys. Chem. C, 112, 6430 – 6438.

3. Bowers, G.M., Bish, D.L., and Kirkpatrick, R.J., 2008, Cation exchange at the mineral-water interface: H_3O^+/K^+ competition at the surface of nano-muscovite, Langmuir, 24, 10240-10244.

4. Bowers, G. M., and Kirkpatrick, R.J., 2009, Natural Abundance ^{43}Ca NMR spectroscopy of tobermorite and jennite: model compounds for C-S-H, J. Am. Ceram. Soc., 92, 545-548.

5. Reinhold, M.X., Babu, P.K., and Kirkpatrick, R. J., 2009, Preferential adsorption of lower-charge glutamate ions on layered double hydroxides: an NMR investigation, J. Phys. Chem. C, 113, 3378-3381.

6. Reinhold, M.X., Babu, P.K., and Kirkpatrick, R. J., 2009, Proton dynamics in layered double hydroxides: a ^{1}H T_1 relaxation and line width investigation, J. Phys. Chem. C, 113, 10623-10631.

7. Wang, J. W., Kalinichev A.G., and Kirkpatrick, R.J., 2009, Asymmetric hydrogen bonding and orientational ordering of water at hydrophobic and hydrophilic surfaces: a

comparison of water/vapor, water/talc, and water/mica interfaces., J. Phys. Chem. C., 113, 11077-11085.

8. Ufimtsev, I. S., Kalinichev, A. G., Martinez, T. J., and Kirkpatrick, R. J., 2009, A multistate empirical valence bond model for solvation and transport simulations of OH^- in aqueous solutions, Physical Chemistry Chemical Physics., 11, 9420-9430.

9. Kalinichev. A.G., Kumar P, P., and Kirkpatrick, R. J., 2010, Effects of hydrogen bonding on the properties of layered double hydroxides intercalated with organic acids: molecular dynamics computer simulations, Philosophical Magazine, 90, 2475-2488.

10. Iskrenova-Tchoukova, E., Kalinichev. A.G., and Kirkpatrick, R.J., 2010, Metal cation complexation with natural organic matter in aqueous solutions: molecular dynamics simulations and potentials of mean force, Langmuir, 26, 15909-15919.

11. Kalinichev. A.G., Iskrenova-Tchoukova, E., Ahn, W.-Y., Clark, M.M., and Kirkpatrick, R.J., 2011, Effects of Ca^{2+} on supramolecular aggregation of natural organic matter in aqueous solutions: a comparison of molecular modeling approaches, Geoderma, 169, 27-32.

12. Bowers, G.M., Singer, J.W., Bish, D.L., and Kirkpatrick, R.J., 2011, Alkali metal and H_2O dynamics at the smectite/H_2O interface, J. Phys. Chem. C, 47, 23395-23407.

13. Bowers, G. M., and Kirkpatrick, R.J., 2011, Natural abundance ^{43}Ca NMR as a tool for exploring calcium biomineralization: renal stone formation and growth, J. Crystal Growth and Design, 11, 5188-5191.

14. Singer, J.W., Yazaydin, A.O., Bowers, G.M., and Kirkpatrick, R.J., 2012, Structure and transformation of amorphous calcium carbonate – a solid-state ^{43}Ca and computational molecular dynamics investigation, Chemistry of Materials, 24, 1828-1836.

15. Morrow, C.P, Yazaydin, A.O., Krishnan, M., Bowers, G. M., Kalinichev, A.G., and Kirkpatrick, R.J., 2013, Structure, energetics, and dynamics of smectite clay interlayer hydration: molecular dynamics and metadynamics investigation of Na-hectorite, J. Phys. Chem. C, 117, 5172-5187.

16. Saharay, M., Yazaydin, A.O., and Kirkpatrick, R.J., 2013, Dehydration-induced amorphous phases of calcium carbonate, J. Phys. Chem. B, 117, 3328-3336.

17. Krishnan, M., Saharay, M., and Kirkpatrick, R.J., 2013, Structure and dynamics of nano-confined CO_2 and poly(ethylene glycol) in montmorillonite composites, J. Phys. Chem. C., 117, 20592 – 20609.

18. Saharay, M., and Kirkpatrick, R. J., 2014, Onset of orientational order in amorphous calcium carbonate (ACC) upon dehydration, Chem. Phys. Letters, 591, 287-291.

19. Bowers, G.M., Singer, J.W., Bish, D.L., and Kirkpatrick, R.J., 2014, Structural and dynamical relationships of Ca^{2+} and H_2O in smectite/^2H_2O systems, American Mineralogist, 99, 318-331.

20. Bowers, G.M., Hoyt, D.W., Burton, S.D., Ferguson, B.O., Varga, T., and Kirkpatrick, R.J., 2014, In situ ^{13}C and ^{23}Na MAS NMR investigation of supercritical CO_2 incorporation in smectite natural organic matter composites, J. Phys. Chem. C, 118, 3564-3573.

21. Saharay, M., and Kirkpatrick, R. J., 2014, *Ab initio* and metadynamics studies on the role of essential functional groups in biomineralization of calcium carbonate and environmental situations, Phys. Chem. Chem. Phys., 16, 26843-26854.

22. Kirkpatrick, R.J. Kalinichev, A.G., Bowers, G. M., Yazaydin, A.O., Krishnan, M., Saharay M., and Morrow, C.P., 2015, NMR and computational molecular modeling studies of mineral surfaces and interlayer galleries, American Mineralogist, 100, 1341-1354, Invited American Mineralogist Centennial Article.

23. Greathouse, J.A., Hart, D.B., Bowers, G.M., Kirkpatrick, R.J., and Cygan, R.T., 2015, Molecular simulation of structure and diffusion at smectite-water interfaces: using expanded clay interlayers as model nanopores, J. Phys. Chem. C, 119, 17126-17136.

24. Bowers, G.M., Argersinger, H.E., Reddy, U. V., Johnson, T.A, Arey, B., Bowden, M., and Kirkpatrick, R.J., 2015, Integrated molecular and microscopic scale insight into morphology and ion dynamics in Ca^{2+}-mediated natural organic matter floccs, J. Phys. Chem. C, 119, 17773-17783.

25. Yazaydin, A.O., Bowers, G.M., and Kirkpatrick, R.J., 2015, Molecular dynamics modeling of carbon dioxide, water and natural organic matter in Na-hectorite, Physical Chemistry Chemical Physics, 17, 23356-23367.

26. Sena, M.M., Morrow, C.P., Kirkpatrick, R.J., and Krishnan M., 2015, Structure, energetics, and dynamics of supercritical carbon dioxide at smectite mineral-water interfaces: molecular dynamics and adaptive biasing force investigation of CO_2/H_2O mixtures nanoconfined in Na-montmorillonite, Chemistry of Materials, 27, 6946-6959.

27. Loganathan, N., Yazaydin, A.O., Bowers, G.M., Kalinichev, A.G., and Kirkpatrick, R. J., 2016, Structure, energetics, and dynamics of Cs^+ and H_2O in hectorite: molecular dynamics simulations with an unconstrained substrate surface, J. Phys. Chem., C, 10290-10310.

28. Reddy, U.V., Bowers, G.M., Loganathan, N., Bowden, M., Yazaydin, A.O., and Kirkpatrick, R.J., 2016, Water structure and dynamics in smectites: X-ray diffraction and ^2H NMR spectroscopy of Mg-, Ca-, Sr-, Na-, K-, Cs-, and Pb-hectorite, J. Phys. Chem. C, 120, 8863-8876.

29. Loganathan, N., Yazaydin, A.O., Bowers, G.M., Kalinichev, A.G., and Kirkpatrick, R. J., 2016, Cation and water structure, dynamics and energetics in smectite clays: a molecular dynamics study of Ca-hectorite, J. Phys. Chem. C, 120, 12429-12439.

30. Bowers, G.M., Schaef, H.T., Loring J.S., Hoyt, D.W., Burton, S.D., Walter E.D., and Kirkpatrick, R.J., 2017, Role of cations in CO_2 adsorption, dynamics, and hydration in smectite clays under in situ supercritical CO_2 conditions, J. Phys. Chem. C, 121, 577-592.

31. Schaef, H.T., Loganathan, N., Bowers, G.M., Kirkpatrick, R.J., Yazaydin, A.O., Burton, S.D., Hoyt, D.W., Ilton, E.S., Thanthiriwatte, K.S., Dixon, D.A., McGrail, B.P., Rosso, and Loring, J.S., 2017, Tipping point for expansion of layered aluminosilicates in weakly polar solvents: supercritical CO_2, ACS Applied Materials and Interfaces, 9, 36783-36791.

32. Saharay, M., and Kirkpatrick, R.J., 2017, Water dynamics in hydrated amorphous materials: a molecular dynamics study of the effects of dehydration in amorphous calcium carbonate, Phys. Chem. Chem Phys., 19, 29594-29600.

33. Loganathan, N., Bowers, G.M., Yazaydin, A.O., Schaef, H.T., Loring, J.S., Kalinichev, A.G., and Kirkpatrick, R.J. 2018, Clay swelling in dry supercritical carbon dioxide: effects of interlayer cations on the structure, dynamics and energetics of CO2 intercalation probed by XRD, NMR, and GCMD simulations, J. Phys. Chem. C, 122, 4391-4402.

34. Bowers, G.M., Loring, J.S., Schaef, H.T., Walter E.D., Burton S.D., Hoyt, D.W., Cunniff, S.S., Loganathan N., and Kirkpatrick, R.J., 2018, Interaction of hydrocarbons with clays at reservoir conditions: *in situ* IR and NMR spectroscopy and X-ray diffraction for expandable clays with variably wet supercritical methane, ACS Earth and Space Chemistry, in press.

35. Nanda, R., Reddy, U.V., Bowers, G.M., Bowden, M., and Kirkpatrick, R.J., submitted, The structural and dynamical role of water in natural organic matter: a ^2H NMR study, Organic Geochemistry.

36. Ferguson, B.O., Arey, B., Varga, T., Burton, S.D., Bowden, M., Argersinger, H.E., Kirkpatrick, R.J., and Bowers G.M., submitted, X-ray diffraction and helium ion microscopy of smectite natural organic matter composites, Clays and Clay Minerals.

37. Loganathan, N., Yazaydin, A.O., Bowers, G.M., Kalinichev, A.G., and Kirkpatrick, R.J., in preparation, Competitive adsorption of H_2O and CO_2 in the interlayers of Cs- and Ca-hectorite using GCMD simulations.

38. Cunniff, S.S., Schaef, H.T., Loring, J.S., Burton, S.D., Walter, E.D., Kirkpatrick, R.J., and Bowers, G.M.. Influence of ion polarizability on the interactions of variably wet supercritical carbon dioxide with smectite clays, in preparation.

39. Loganathan, N., Yazaydin, A.O., Bowers, G.M., Kalinichev, A.G., and Kirkpatrick, R.J.

Understanding the hydrophilic and hydrophobic interactions of NOM at hydrated clay surfaces: a molecular dynamics study, in preparation.

40. Bowers, G.M., Loganathan, N., Ferguson, B.O., Reddy, U.V., Argersinger, H.E., Johnson, T.A., Arey, B., and Kirkpatrick, R.J.. Smectite-natural organic matter interactions in Ca^{2+} bearing systems on the molecular scale, in preparation.

II. Highlights of Recent Research

A. Clay-Water Systems

Expandable clay minerals (smectites and smectite interlayers in mixed layer clays) are ubiquitous in soils, sediments and sedimentary rocks and play central roles in controlling their chemical and physical behavior. The surfaces and interlayers of these materials are structurally disordered, and atoms and molecules associated with them have dynamics with frequencies that span many orders of magnitude. They readily hydrate and dehydrate depending on the activity of water, and water incorporation into their interlayers is central to their properties. It is now also well-established that smectite interlayers can, in some circumstances, incorporate CO_2 at temperatures and pressures relevant to the geological subsurface. The combination of laboratory experiments and computational molecular modeling is uniquely capable of investigating the molecular scale structure, dynamics and energetics of fluids at external and interlayer smectite surfaces. In particular, the combination of modeling and NMR spectroscopy provide access to dynamical reorientation rates over more than 10 orders of magnitude. Likewise, the element-specific molecular-scale structural information provided by NMR is directly complimentary to computational modeling, providing structural information about the bulk material or its individual atomic and molecular components.

Our work on clays began with hydrous systems, with focus on the structure and dynamics of the exchangeable cations and water molecules, and progressed to clay-NOM interactions in hydrous systems and then to clay-CO_2±NOM and clay-CH_4 systems. We also published review and synthesis papers related to clay systems. Kirkpatrick et al. (paper 22, Table 1) highlights the complementarity between NMR and computational modeling and reviews the research on smectites and other layer structure materials. Greathouse et al. (paper 23, Table 1) discusses the ability of computational molecular modeling using the current generation of supercomputers to effectively address meso-scale fluid-solid systems with pore sizes approaching 10 nm. Our more recent papers on molecular modeling of Ca- and Cs-hectorite also demonstrate this capacity (papers 27 and 29, Table 1)

For hydrous smectite systems, our paper on Na-hectorite (paper 15, Table 1) used classical and enhanced (metadynamics) MD methods to investigate interlayer structure and energetics in the stable 1 and 2-layer hydrates of Na-hectorite. The results are in good agreement with our previous experimental NMR results for this phase (paper 12, Table 1) and provide an important reference with which to compare the behavior and properties of smectites containing other cations and CO_2. The calculations provide detailed information about the variation in water-cation coordination, H-bond structure, cation and water diffusion, and the energetics of water site hopping. Importantly, they confirm our interpretation of ^2H NMR results for this phase that the interlayer water molecules

undergo simultaneous rapid rotational motion about their C_2 symmetry axis (molecular dipole, Figure 1) and site hopping with C_3 symmetry with a well-defined average angle (ω) of ~52° between the molecular dipole axis and the basal surface of the clay.

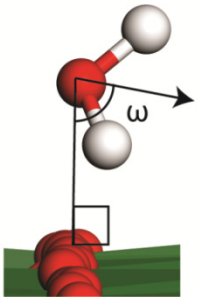

Figure 1. The definition of the angle ω between the normal to the basal surface of a clay and the orientation of the dipole axis of a water molecule. ^{2}H NMR and computational molecular modeling results show that for clay interlayers the water molecules are undergoing rotation around the dipole axis at frequencies >$2x10^7$ Hz and that on average this axis undergoes hopping with C_3 symmetry around the normal to the basal surface at frequencies >$2x10^6$ Hz.

Variable temperature and variable relative humidity ^{43}Ca and ^{2}H NMR results for isotopically enriched ^{43}Ca-hectorite with ^2H_2O (paper 19, Table 1) and for ^2H_2O in Cs-, Sr-, Ca-, Mg-, and Pb-hectorite (paper 28, Table 1) extend the experimental basis for understanding the effects of cation hydration energy and polarizability on interlayer structure and dynamics in smectite systems. The results show that not just increasing hydration energy but also increasing cation polarizability cause decreasing rates of exchange of water molecules between sites coordinating the interlayer cation and those coordinating only the basal surface. This behavior is reflected in the increasing temperature of the transitions between rigidly held and anisotropically averaged water molecules and between anisotropically and isotropically averaged water molecules with increasing hydration energy and polarizability. For instance, for Mg-hectorite equilibrated at 43% R.H., at 298 and 313K the ^{2}H NMR spectra (Figure 2A) contain one quadrupolar-split ^{2}H resonance representative of interlayer ^2H_2O undergoing anisotropic dynamics at frequencies >~10^6 Hz. The line shape and splitting of the two singularities are consistent with the combined H_2O rotation-hopping model. The presence of only one resonance indicates rapid exchange and spectral averaging of ^2H_2O in nearest neighbor coordination to the Mg and ^2H_2O not coordinated to it. At 233 and 253K, the spectrum contains two resonances, a narrow peak in the center representing ^2H_2O molecules not coordinated to Mg that are undergoing isotropic reorientation, and the quadrupolar split resonance (the two singularities on either side) representing water molecules coordinated to Mg^{2+} and undergoing the C_2/C_3 motion. The two components are resolvable at these temperatures because the frequency of exchange between sites coordinated to Mg and not coordinated to it has fallen below ~10^4 Hz. This behavior cannot be due to tetrahedral jump behavior, such as that in ice 1-h, because this type of motion does not occur in the interlayer galleries. The poorly resolved spectrum at 273K occurs because water molecules are exchanging between these two types of sites at frequencies of the order of 10^3 Hz. Mg^{2+} is the only cation for which this behavior is observed, because its high hydration energy (ΔH_{hydr}= 1907.5kJ/mol) results in relatively long residence times for ^2H_2O in nearest neighbor coordination to the cation. At 173K and 193K, the broad quadrupolar resonance with maxima near ±70 kHz represents rigidly held ^2H_2O molecules, and the broad but symmetrical peak in the center represents such molecules undergoing reorientation at frequencies of the order of 10^5 Hz. These are probably ^2H_2O molecules not coordinated to Mg^{2+}. The spectrum at 213K is transitional. The magnitude of the ^{2}H NMR quadrupolar coupling constant is well known to be proportional to the hydrogen bond strength (similar to the O-H stretching frequency observed by vibrational spectroscopy), and the results show that the H-bond strengths of rigidly

held water molecules in hectorite interlayers (H-bond donation between H_2O molecules and from H_2O molecules to basal oxygens) are similar to those in ice-1h. XRD shows that ice is not present for this sample at any temperature.

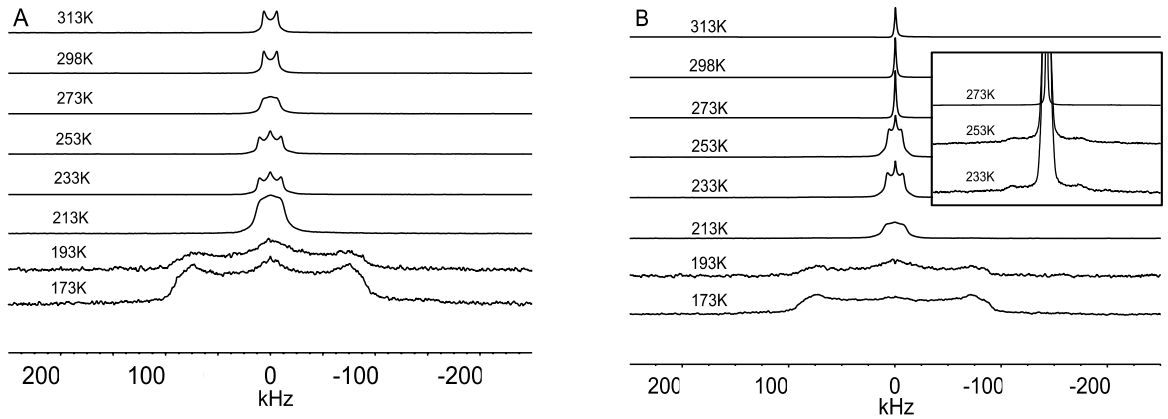

Figure 2. Static ^2H NMR spectra of Mg-hectorite equilibrated at 43%R.H. (A) and 100% RH. (B) and collected at the indicated temperatures. See text for spectral interpretation.

The ^2H NMR spectra of Mg-hectorite equilibrated over ^2H_2O at 100% R.H. shows generally similar behavior except at temperatures of 273K and above, where there is only one narrow resonance representing isotropically averaged water molecules (Figure 2B). This resonance represents all the water molecules in the sample and indicates that at large interlayer water contents there is complete rotational and site exchange dynamics at frequencies $>\sim 10^5$ Hz. At 173K and 193K, the broad quadrupolar resonance with maxima near ±70 kHz also contains signal for ice-1h, which XRD shows to be present at this R.H. and temperature range.

More recently, our MD modeling of Ca- and Cs-hectorite (papers 27 and 29, Table 1) has expanded on the modeling for Na-hectorite and provides a more detailed molecular scale picture of the experimental ^2H NMR results for these phases. The results highlight the effects of their very different hydration energies [-283 kJ/mol for Cs^+ and -1,592 kJ/mol for Ca^{2+}) on the interlayer structure, energetics and dynamics of smectites and also on the structural arrangement of the cations on the external surfaces. For Ca-hectorite, the results show stable monolayer and bilayer hydrates and expansion to higher hydrates at large humidities, consistent with XRD and NMR results from the current grant period (paper 14, Table 1). In the two-layer hydrate, interlayer Ca^{2+} ions occur in outer sphere coordination and are 8-coordinated by H_2O in a square antiprism (Figure 3b), consistent with the ^2H NMR results. In contrast, the results show that Cs-hectorite occurs only as a monolayer hydrate, in agreement with experiment, and that the interlayer Cs^+ occurs in inner sphere coordination with the basal surface either above the ditrigonal cavities of the basal surface or above individual Si-tetrahedra (Figure 3a). These results support the interpretation of our ^2H_2O NMR results for Cs-hectorite that indicate larger average ω angles of about 67° than for bilayer hydrates with other cations. Interlayer H_2O molecules in Ca-hectorite diffuse more slowly than in Na- and Cs-hectorite interlayers at all hydration states, reflecting its larger hydration energy. In parallel, the site residence times for H_2O molecules in nearest neighbor coordination to Ca^{2+} in hectorite interlayers are approximately eight times longer than in coordination to Cs^+ in Cs-hectorite and three times longer in H-bond coordination to the basal oxygens of the clay.

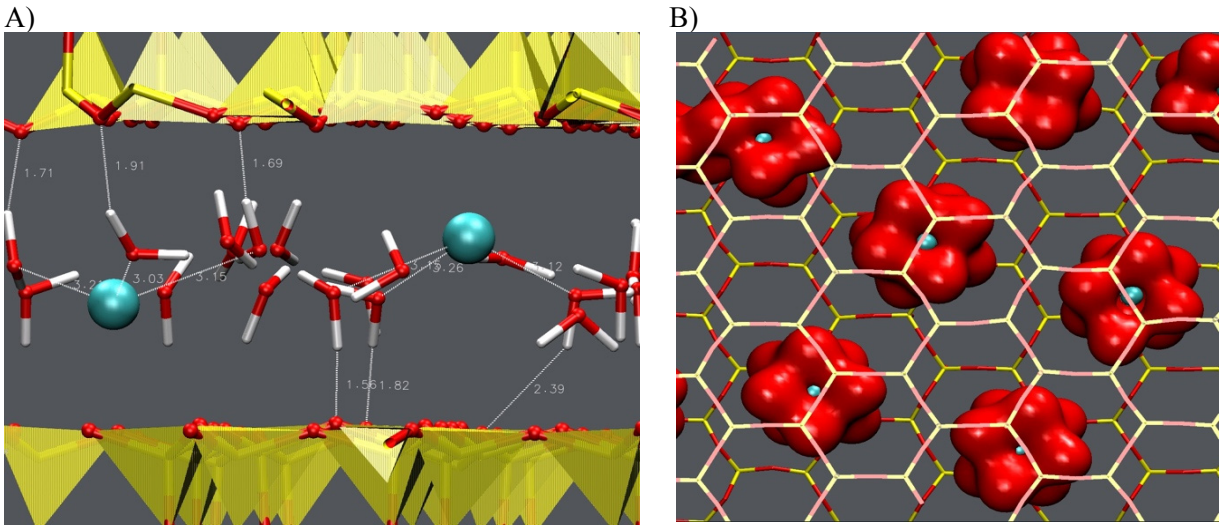

Figure 3: Images from MD simulations of H_2O molecules hydrating the basal surface and cations in A) the stable monolayer hydrate of Cs-hectorite viewed parallel to the clay surface showing the inner sphere Cs^+ coordination, and B) the stable bilayer hydrate of Ca-hectorite viewed perpendicular to the surface showing the outer sphere cubic antiprism Ca^{2+} coordination by H_2O. For clarity only H_2O molecules coordinated to the metal ions are shown. Yellow – Si or basal Si tetrahedra, blue balls – Cs^+ / Ca^{2+} ions. In a) red sticks – O_{H2O}, white sticks – H_{H2O}. In b) red sticks – basal oxygens, red balls H_2O molecules coordinated to Ca^{2+} ions.

B. Hydrated Natural Organic Matter (NOM) and Cation-NOM Floccs

NOM is a complex mixture of organic molecules formed in nature by the weathering of principally plant materials. It is ubiquitous in natural waters and soils and plays a wide variety of important roles in controlling the physical and chemical properties of these natural systems. It greatly influences such properties as soil structure and water retention, the sequestration and mobilization of many organic and inorganic species, and the oxidative or reductive transformation of organic molecules. It can also play an important role in the fouling of water filtration membranes. Chemically and structurally, NOMs are very complex and are typically composed of substituted aromatic and aliphatic structural elements. Interaction among individual NOM molecules is thought to be mediated by intramolecular interactions, including hydrophobic effects and cation bridging. NOMs are typically classified based on empirical solubility behavior, with fulvic acid (FA) soluble at all pH values, humic acid (HA) soluble only in alkaline solutions, and humin insoluble at all pHs. NOMs contain many kinds of functional groups, with FAs typically having more oxygen-bearing groups than HAs. For most NOMs, carboxylic sites are the dominant reactive functional group, with phenolic and alcoholic sites also important. N- and S- sites are also present but at lower abundances.

Water plays a wide variety of critical roles in controlling the properties of NOM. These including its swelling behavior and interaction with dissolved species (e.g., ion retention and transport

properties), the interaction of NOM molecules with each other, and the behavior of NOM aerosols in the Computational molecular modeling has suggested that hydrophobic interactions, water molecule bridging, cation bridging, cation hydration, and H-bonding all contribute to the interactions among NOM, water, dissolved ions, and mineral surfaces. For instance, MD simulations of graphene and functionalized graphene (model materials for the aromatic components of NOMs) show that the sheets of the non-functionalized form tend to aggregate parallel to each other, whereas the functionalized form, which can H-bond to water molecules, are better dispersed.

There are, however, few studies of the molecular scale structure, dynamics, and energetics of water and cations in NOM. With support from this grant, we undertook a sequence of experimental and computational studies to address these issues (papers 10, 11, 20, 24, 25, 35, 39, 40, Table 1). Experimental methods included variable temperature and humidity ^{2}H and ^{43}Ca NMR spectroscopy, He ion microscopy (HeIM), scanning electron microscopy (SEM), and thermogravimetric (TGA) analysis to probe water and cation behavior in as-received (cation-free) and ^{43}Ca-exchanged Suwannee River NOM and its fulvic acid and humic acid fractions as functions of pH. pH controls the charge on the NOM through protonation-deprotonation reactions. As for the clays discussed above, ^{2}H and cation NMR provide direct, element-specific information about structure and dynamical behavior. HeIM provides significantly enhanced image resolution and depth-of-field compared to SEM due to the larger number of secondary backscattered electrons produced by the heavy helium ion and is proving to be a very effective tool for examining mineral-NOM systems (Figure 4). For these samples, HeIM shows a rich, multi-scale diversity of morphologies that are based on building blocks ~10 nm in diameter. This size is comparable to the radius of gyration of individual Suwannee River molecules in solution determined by small-angle X-ray scattering.

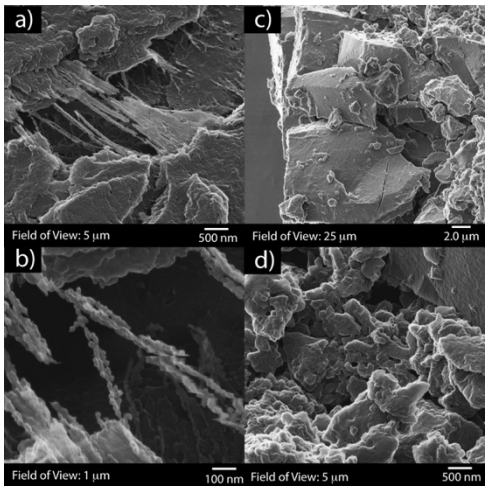

Figure 4. Helium-ion microscopy images of Ca-NOM formed at ~pH 12. Flocculated NOM is dominated by massive aggregates (c) and globular morphologies (d) that appear to be assemblages of ~10 nm spherical particles ("string of pearls" filaments) illustrated in a) and b).

The ^{43}Ca NMR results for NOM samples equilibrated at 100% R.H. over 99% isotopically enriched $^{2}H_2O$ shows that both the ionic strength and the protonation state of the reactive functional groups of the NOM affect Ca^{2+} binding and dynamics (paper 28, Table 1), as suggested by previous MD results (e.g., paper 10, Table 1. The data show a wide range of Ca^{2+} binding environments in floccs formed from Ca^{2+}/NOM solutions. There are two distinct populations of Ca^{2+} environments in samples made at low pHs (Figure 5), where all the carboxylic, phenolic, and amine functional

groups are protonated. For samples made at high pHs, where the carboxylic and phenolic functional groups are deprotonated, this is a more continuous set of local environments. The ^{43}Ca chemical shifts indicate that the Ca-O bond distances are shorter and the Ca-O coordination numbers are lower under basic conditions with deprotonated functional groups and that the dynamics of this population is dominated by relatively slow exchange between NOM-associated Ca^{2+} binding environments. Near room temperature, samples with excess Ca^{2+} equilibrated at 100% R.H. show substantial ^{43}Ca line narrowing, indicating site exchange at frequencies $>\sim10^4$ Hz when the water content of the NOM is large. Our MD simulations of NOM in aqueous solution support this interpretation, showing site exchange frequencies of $\sim10^9$ -10^{10} Hz for Ca^{2+} coordinated to $-COO^-$ sites (paper 10, Table 1). At low temperatures with excess Ca^{2+} present, the dynamics reflects strong association of the Ca^{2+} with the NOM due to ion exclusion by ice-1h.

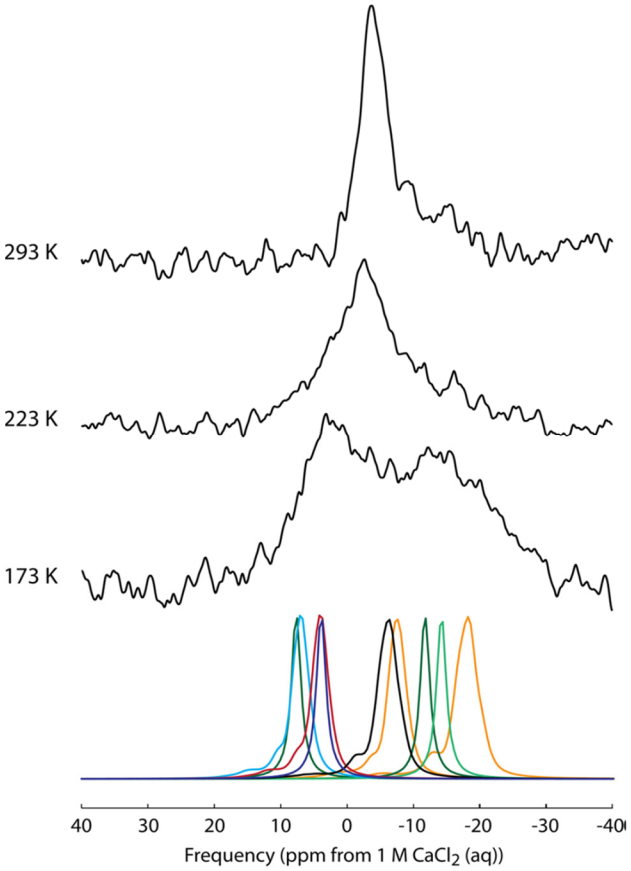

Figure 5. ^{43}Ca MAS NMR spectra at 20.0 T for Ca-humic acid floccs made at pH 2 equilibrated at 100% relative humidity as a function of temperature compared to simulations of the 20.0 T spectra of known Ca-organic salts (bottom row) calculated based on the parameters of Wong et al. (2006, 2008). Orange is Ca-citrate tetrahydrate, light green is Ca-ascorbate dihydrate, dark green is Ca-acetate monohydrate, cyan is Ca-D-gluconate pentahydrate, red is Ca-formate, black is Ca-oxalate trihydrate, and blue is Ca-succinate monohydrate. There are two groups of Ca-organo salts; a high-frequency group with a mean Ca−O distance of 2.41 Å and a low-frequency group with mean Ca−O distance 2.47 Å. The two peaks for Ca-HA-pH 2 peaks at 173 K span the full chemical shift range of both groups of model compounds and are centered among the two groups. At higher temperatures, the Ca^{2+} ions in the NOM undergo dynamical averaging via exchange through the water in the NOM.

The variable temperature and variable R.H. (43% and 100%) ^{2}H NMR results for as-received Suwannee River NOM, HA, and FA without exchangeable cations shows the presence of multiple ^{2}H environments and complex dynamical behavior. For room temperature samples hydrated in ^2H_2O and then dehydrated, the spectra distinguish ^{2}H exchanged onto carboxylic sites of the NOM that does not undergo rapid reorientation at frequencies $>\sim10^3$ Hz, ^{2}H exchanged onto phenolic and alcohol sites of the NOM that undergoes rapid but anisotropic dynamical reorientation at frequencies $>10^5$ Hz, and a small number of residual ^2H_2O molecules that are in rapid, isotropic reorientational motion at frequencies $> 10^5$ Hz. For samples exposed to water and not dried, XRD results collected at temperatures from 173 to 298 K show the formation of ice-1h in samples exposed to 100% R.H. but not in samples exposed to 43% R.H.

Near room temperature, the ^2H NMR spectra of these samples all contain a narrow resonance for mobile water undergoing rapid isotropic motion, and a broader symmetrical resonance probably due to a combination of more dynamically restricted water molecules and ^2H exchanged onto phenolic and alcohol functional groups undergoing rapid anisotropic motion. The 43% R.H. samples also yield a broader quadrupole dominated resonance for ^2H exchanged onto carboxylic groups (Figure 6A). The relative intensity of the resonance for this site increases from HA to NOM to FA (Figure 6B), reflecting the increasing concentration of carboxylic sites from HA to FA (the NOM sample used here has an HA/FA ratio of approximately 4/1). With decreasing temperature, the resonances for dynamically restricted water molecules and ^2H exchanged onto phenolic and alcohol functional groups becomes broader, reflecting a decreasing rate of ^2H exchange between the water molecules and functional groups and a decreasing rate of reorientation of the ^2H_2O molecules. The formation of ice-1h is directly reflected in the ^2H spectra of the 100% R.H. samples as a resonance with a quadrupole coupling constant (QCC) of ~ 180 kHz. The QCC for these sites is somewhat less than the value of 216 kHz for bulk ice-1h, probably because a small crystallite size in our samples results in many molecules being near the surface. ^2H near crystallite surfaces would see a range of electric field gradients different than in bulk ice. For the 43% R.H. samples, which do not contain ice-1h, there is also a broad, poorly resolved resonance with QCCs of ~ 180 kHz for which the relative signal intensity increases with decreasing temperature. This signal represents ^2H_2O molecules that are not crystallized in ice-1h but have greatly reduced reorientation frequencies at low temperature. Such molecules are likely to be present in the 100% R.H. samples also, but they cannot be resolved. As for similar sites in clay interlayers, the decreased frequency of motion of these molecules at low temperatures is probably due to H-bonding. As discussed above, for rigidly held ^2H_2O molecules, the QCC is well known to correlate with H-bond distance. For the ^2H_2O molecules in our NOM, the QCC of ~180 kHz implies an average O-H···O distance of approximately 2.7 Å. The absence of well-defined singularities for the undried samples suggests that there is a range of H-bond distances contributing to the reduced spectral resolution. At both R.H.s, some of the ^2H_2O molecules do not freeze and retain their isotropic motion even at 173K, the lowest temperature

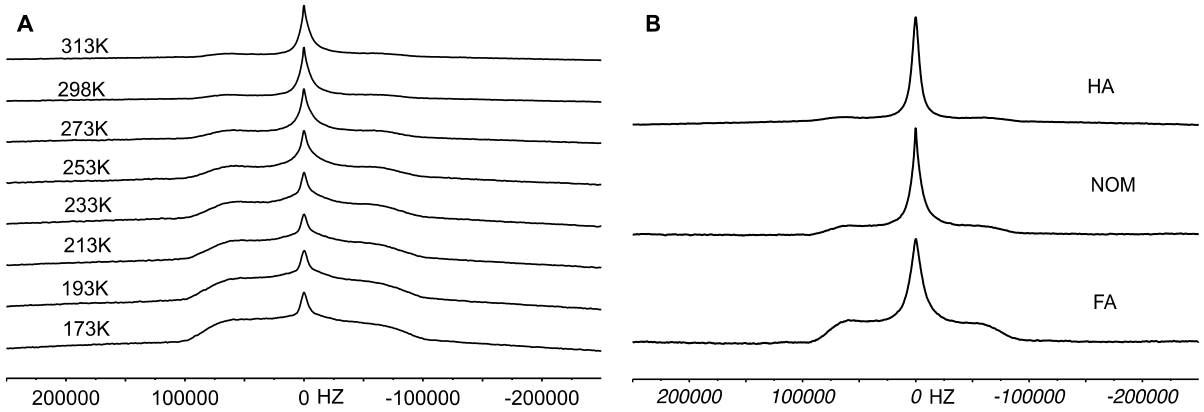

Figure 6. ^2H NMR spectra of A) NOM equilibrated at 43% R.H. and collected at the indicated temperature, and B) HA (top), NOM (middle), and FA (bottom) equilibrated at 43% R.H. and collected at 298K.

investigated. We assign these to water molecules that do not participate significantly in H-bonding. These molecules are probably located in positions associated with hydrophobic environments and may be trapped near aromatic or aliphatic moieties.

C. Clay-NOM Composites

NOM interaction with mineral surfaces is thought to play a significant role in many geochemical processes in near-surface environments, including binding and transport of many chemical species. The molecular scale interactions that control the binding of NOM to mineral surfaces is thought to be dominated by hydrophobic interactions at low pHs where the functional groups of the organic matter are protonated, with cation bridging and multi-layer (DLVO) effects playing more important roles at neutral to high pHs where many of the critical functional groups are deprotonated. In many respects, important aspects of NOM-mineral interactions, such as the effects of different cations; the role of water molecules and H-bond interactions; and the detailed structure, dynamical behavior, and energetics at the interface remain poorly understood.

We prepared composites of hectorite and Suwannee River NOM and its FA and HA components at acidic and basic pHs (~ 2 and 12) and characterized them using X-ray diffraction, SEM/energy dispersive X-ray composition analysis, and HeIM. To our knowledge, this is the first HeIM study of clays and clay-NOM composites. The results show that NOM is not incorporated into the smectite interlayers. Rather, at basic pHs, it forms relatively thin (< 1 μm) coatings on the external surfaces of packets of platelets. The structural details of these coatings (e.g. coating thickness) is likely influenced by DLVO stabilization of NOM in solution and the relative ability of the ion to form bridges between two NOM molecules and between NOM and the mineral surface. In contrast, at acidic pHs the coatings are much thicker on average (up to 3 μm in the Ca-hectorite system) and have a complex morphology with many different types and size-scales of bumps, ridges, and faceted surfaces (Figure 7). Behavior under acidic conditions is probably dominated

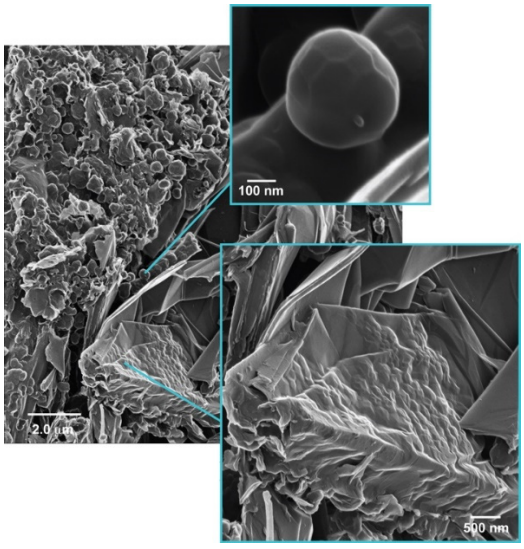

Figure 7. Images of Ca-hectorite-NOM composites prepared at pH 2. The sheet-like foils are smectite packets, and the hummocky and faceted objects are coatings and particles of pure NOM.

observations are consistent with the dominance of hydrophobic interactions in NOM aggregation but also suggest that there is a small amount of cation bridging. These results together with our

by hydrophobic interactions and rapid precipitation of NOM from solution. For the most part, the alkali metals appear to have little influence on the morphology of NOM-smectite composites. In contrast, Ca^{2+}, which is known to interact strongly with NOM, causes formation of NOM floccs at acidic pHs that then agglomerate onto the clay surfaces. This result is consistent with our MD modeling that shows strong Ca^{2+}-NOM interactions (paper 10, Table 1) and our more recent results that show that Ca^{2+} causes extensive aggregation of NOM molecules near smectite surfaces (Figure 8; paper 36, Table 1). XRD results show that the NOM coatings stabilize interlayer H_2O, with the clay-NOM composites generally exhibiting larger basal spacings indicative of excess interlayer H_2O than the corresponding base clay under similar R.H. conditions; none of the basal spacings are large enough to suggest NOM enters the clay interlayers. These observations are consistent with the known ability of NOM to sorb and retain water in soils.

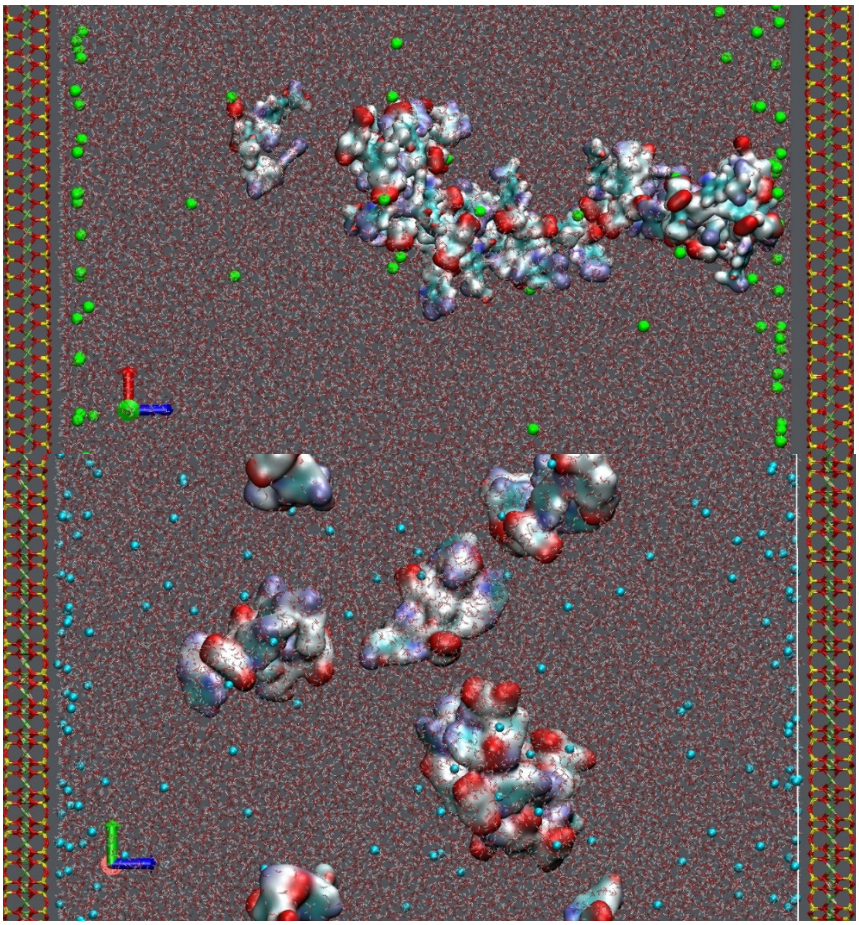

Figure 8. Snapshots from MD simulations of the H_2O-NOM-hectorite systems (~80,000 atoms) with Ca^{2+} (top) and Cs^{+} (bottom) as the charge balancing cations. Each simulation modeled a meso-pore 15 nm thick between two clay basal surfaces with 16 TNB NOM molecules and 50 molecular layers of H_2O. The lateral dimensions (L_x and L_y) of the system corresponds ~75Å each. The simulations were run for ~70 ns. Color Labels: Yellow -Si, Red (surface) – Surface O, Green – Ca^{2+} ions, Light Blue – Cs^{+} ions, NOM molecules are represented as aggregated surface. white regions – H (NOM), cyan regions – C(NOM), red regions -O(NOM), blue regions -N(NOM). H_2O molecules are represented in transparent

mode for clarity.

Variable temperature ^{43}Ca NMR spectroscopy of the Ca-hectorite-NOM composites shows that the NOM fraction (HA, FA, or NOM), preparation pH, and ionic strength have little influence on the binding and dynamics of Ca^{2+} (paper 20, Table 1). These NMR results suggest that a majority of the Ca^{2+} is associated with environments similar to those of base Ca-hectorite; most likely fully hydrated Ca^{2+} ions in the interlayers or within ~5 Å of the clay external surfaces. However, the composites all exhibit ^{43}Ca NMR resonances with a consistent displacement to more negative chemical shifts and slightly greater linewidths with respect to base Ca-hectorite. The magnitude of the shift and linewidth increase are independent of pH, NOM fraction, or ionic strength. These ^{43}Ca NMR data for a Ca-oxalate based renal stones (paper 13, Table 1) suggest that small chemical shift changes may be diagnostic of Ca^{2+} bridging between inorganic surfaces and organic molecules in inorganic/organic hybrid materials.

Computational MD modeling provides a more detailed picture of these interactions. Calculations of NOM binding to the exterior surfaces of Na-hectorite using the standard TNB model for NOM shows that at near-neutral pH conditions (carboxylic groups deprotonated, phenolic and amine groups protonated) Na^+ does not bridge the NOM to the clay surface and the NOM molecules along with their charge balancing Na^+ ions drift into the aqueous fluid (paper 25, Table 1). Detailed analysis of the NOM aggregate structures shows that their aggregation in solution is driven not by Na^+ bridging between the molecules but by hydrophobic interactions between them. Energetically, hydration of the net-charge neutral Na-NOM molecules and molecular aggregates outweighs the sum of their Coulombic and dispersive interactions with the net-charge neutral Na-clay particle and the interactions of the water molecules with the hydrophobic structural elements of the NOM.

Larger MD simulations of hectorite-H_2O-NOM systems (~80,000 atoms) with Ca^{2+} and Cs^+ as the charge balancing cations and with more NOM molecules in a meso-scale pore ~15 nm thick further illustrate the effects of cation hydration energy on mineral-NOM systems (Figure 8). These simulations were allowed to evolve for ~70 ns in order to probe the effect of cations in bringing the NOM molecules closer to the surface and to investigate the structure and dynamics of aggregated NOM molecules. With Cs^+, the NOM molecules form small clusters (typically 2 or 3 individual molecules) that remain in the solution and do not associate with the clay surface even for a short time. In contrast, with Ca^{2+} most of the NOM molecules form a single large cluster that is bound to the clay surface at one end by cation bridges. This behavior is consistent with the known affinity between Ca^{2+} and NOM. The part of the large NOM cluster that is not coordinated to the surface oscillates continuously towards and away from the center of the pore and the surface. With Ca^{2+}, the linkages between the individual NOM molecules in the large cluster occur through both their coordination with Ca^{2+} at the deprotonated carboxylic sites and hydrophobic interaction among the molecules. With Cs^+, on the other hand, formation of the small clusters is driven by principally hydrophobic interactions. The results with Ca^{2+} suggest that the complex, hummocky morphology observed for NOM on hectorite surfaces with Ca^{2+} is due to the formation of relatively large NOM clusters and the direct binding of these clusters to the surface. In contrast, the smoother NOM morphologies observed with the alkali cations appear to be due to layering of smaller clusters of NOM molecules onto the clay surface during sample drying. These simulations also highlight the effects of cation charge and hydration energy on their association with clay surfaces. Most of the Ca^{2+} ions not associated with the NOM molecules lie close to the clay surface in outer

sphere coordination. In contrast, the Cs^+ ions are more uniformly distributed in the solution in the meso-pore, and those that are near the surface occur in inner sphere and outer sphere coordination and also separated from the surface by more than one water molecule. Similar differences also affect the incorporation of CO_2 and CH_4 in smectite interlayers, as discussed below.

D. Clay-scCO_2 Interactions

The interaction of supercritical CO_2 (scCO_2) with mineral surfaces and interlayers is central to understanding the behavior of CO_2 in flooding for enhanced petroleum recovery, geological CO_2 sequestration, and for developing novel CO_2-based fracking technologies. This topic has been of substantial research interest in recent years, but many questions remain about the molecular-scale binding environments, dynamics, and chemical and physical parameters that control CO_2-smectite interactions. In conjunction with our collaborators at PNNL, we have undertaken a program of combined experimental and computational research to investigate CO_2 interactions with clay minerals at geologically relevant conditions (P_{fluid} = 90 bars, T = 323K, equivalent to ~ 1 km depth; papers 17, 20, 25, 26, 30, 31, 33, 37, and 38, Table 1).

The experimental work has utilized novel *in situ* high pressure and temperature magic angle spinning (MAS) NMR, IR, and X-ray diffraction capabilities at PNNL. The NMR system allows fluid pressurization of MAS rotors at temperatures and pressures in the supercritical regime for CO_2 and CH_4. Isotopically enriched $^{13}CO_2$ and $^{13}CH_4$ are necessary for adequate signal/noise ratios during short acquisition periods that permit greater time sensitivity to any chemical reactions and also provide detection of ^{13}C signal from essentially only atoms originally in the pressurizing gas. Importantly, once the rotor is pressurized, it can be used in any NMR spectrometer equipped for solids analysis with a variable temperature controller. We typically use the 300 MHz, 500 MHz, and 850 MHz instruments in the EMSL user facility at PNNL for high pressure NMR. Recent innovations provide so-called one-way pressurization that allows determination of the masses of the solid phases, H_2O, and pressurization fluid (CO_2 and CH_4) in the rotor. This is necessary for detailed quantitative analysis of the data, as illustrated in our recent paper describing the structure and dynamics of CO_2 molecules in smectite interlayers (paper 30, Table 1). (Loring et al. 2012, Schaef et al. 2012, Miller et al. 2013, Schaef et al. 2015). The XRD system is based on a Bruker D8 Discover instrument and subjects a specialized sample holder to an intensely focused 0.5 mm X-ray beam. The system is capable of flowing supercritical fluid with variable and controlled water content (R.H.) through the cell with the R.H. monitored by an online Bruker IR Tensor 27 spectrometer. The PNNL facilities also include *in situ* high pressure and temperature powder X-ray diffraction and infrared (IR) instrumentation that allow for direct comparison to the NMR results.

The computational modeling studies related to these experiments have used classical and biased force field MD methods and more recently a Grand Canonical Molecular Dynamics (GCMD) approach. GCMD combines MC and MD by sampling insertion and deletion of molecules at each MD step to allow simultaneous calculation of equilibrium compositions and system dynamics. Allowing for lateral displacement of the clay layers parallel to each other was essential in this implementation. As with our other studies, the GCMD results provide detailed energetic insights and information about the binding, dynamics, and basal spacing of clays in contact with supercritical fluid phases of varying R.H.

An integrated data set of ^{13}C, ^{43}Ca, ^{23}Na, and ^{133}Cs MAS NMR spectra, IR spectra, and XRD patterns for hydrated Cs-, Na-, and Ca-hectorite exposed to $scCO_2$ at 90 bar and 323K (paper 30, Table 1) demonstrate the importance of the charge balancing cation in controlling the CO_2 adsorption and dynamics as a function of the supercritical fluid R.H. The results show that CO_2 enters hectorite interlayers under different conditions and to different extents depending on the properties of the charge-balancing cation and is a maximum when the basal spacing approaches that of a one water layer (1WL) hydrate. Together, the IR, XRD, and NMR data show that with Cs^+, CO_2 enters the interlayer of dry hectorite and that much of it is retained even when in contact with a water saturated $scCO_2$ phase. In contrast, with Ca^{2+}, significant interlayer adsorption of CO_2 requires that enough H_2O is present to produce a basal spacing approaching that of a ~1WL structure. In Ca-hectorite, the interlayers scavenge H_2O from the supercritical fluid even at water-undersaturated conditions, and the fraction of interlayer-adsorbed CO_2 decreases significantly with increasing R.H., although some CO_2 remains in the interlayer even at 100% R.H. The cation NMR data also show nearest neighbor ion-CO_2 association in Cs-hectorite but not in Ca-hectorite.

The ^{13}C MAS NMR data provide specific structural and dynamical information about the interlayer CO_2 as well. The observed spinning sideband patterns show the presence of anisotropically reorienting CO_2 molecules (Figure 9). We interpret these results to indicate that CO_2 adsorbed in 1WL-type interlayers reorients rapidly ($\nu > 10^5$ Hz) about an axis perpendicular to the clay basal

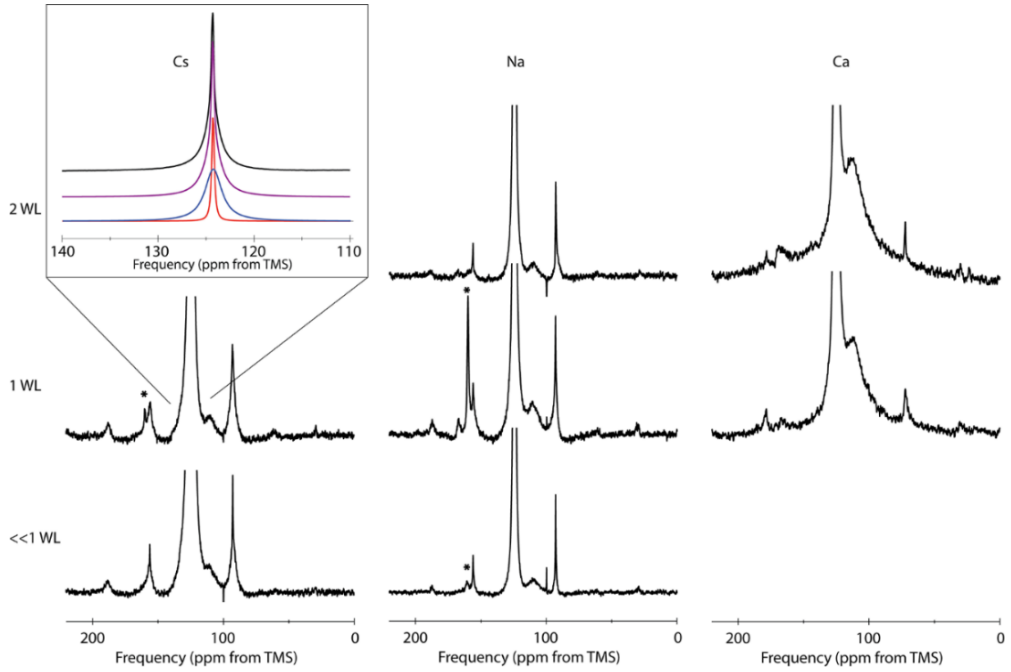

Figure 9. ^{13}C MAS NMR spectra of Cs-hectorite, Na-hectorite, and Ca-hectorite equilibrated at initial humidities designed to produce basal spacings of the type shown on the far left of each row. The spectra were acquired at T = 50°C and P = 90 bars with the 1-way rotor loading system. The narrow component of the individual sidebands in the narrower sideband manifold represent CO_2 adsorbed on external surfaces where they have more dynamic degrees of freedom with respect to the angle with the basal surface. The broader component of the individual sidebands in the broader manifold represent CO_2

adsorbed in 1WL-type (~12.2 Å basal spacing) clay interlayers. Cations with low charge density and large radii (here Cs^+) favor interlayer CO_2 adsorption, and those with higher charge density and smaller radii (here Na^+) favor interlayer hydration and exclusion of CO_2 onto external surfaces.

surface, with the long axis of the CO_2 molecule on average parallel to the basal surfaces. This is in agreement with our MD simulations (paper 26, Table 1) and more recent GCMD modeling of hectorite with dry interlayer CO_2 (paper 33, Table 1) that confirm that the CO_2 molecules undergo rapid rotation about the axis perpendicular to their O-C-O axis and that their average orientation is parallel to the basal surfaces. However, the MD and GCMD results also show that the CO_2 molecules wobble between two surfaces as much as ±30° relative to the surface normal (Figure 10). The experimental ^{13}C NMR data for 2WL-type interlayers (~15 Å basal spacing) show that the signal for interlayer CO_2 is either not visible due to reduced CO_2 incorporation or that this CO_2 experiences reorientational dynamics similar to the 1WL-type case. CO_2 adsorbed on external surface shows similar dynamics, but is able to sample a greater range of angular orientations with respect to the clay basal surface, leading to narrower resonances and spinning sideband patterns compared to CO_2 confined in the interlayer. The ^{13}C NMR peak areas combined with the known clay/H_2O/CO_2 ratio in the NMR rotors allows us to constrain the fraction of scCO_2 adsorbed in each environment and the mole fraction of CO_2 in the interlayer fluid.

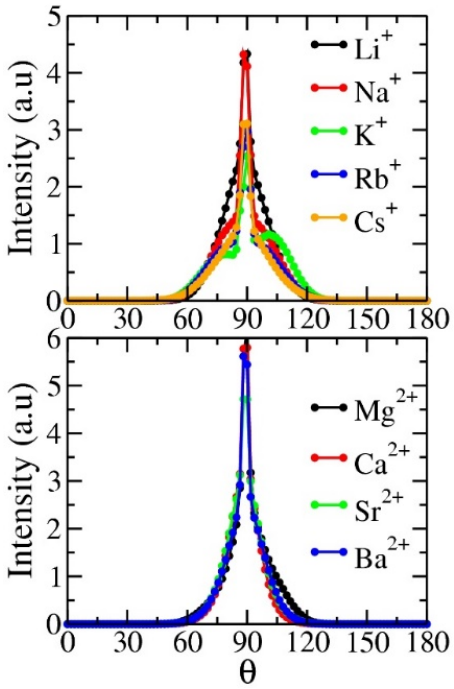

Figure 10**.** Computed orientation distributions of intercalated CO_2 molecules in the interlayers of hectorite at monolayer distances under 323 K and 90bar conditions with different charge compensating cations. θ is the angle between the O-O vector of the CO_2 molecules and the normal to the hectorite basal surface. Top panel – monovalent cations: Bottom panel – Divalent cations.

Our recent integrated experimental and GCMD computational modeling studies of

montmorillonite (paper 31, Table 1) and hectorite (paper 33, Table 1) with a range of interlayer alkali and alkaline earth cations in contact with dry $scCO_2$ are fully consistent with the interpretations of the experimental data above and provide a detailed structural and energetic basis for the results. For example, the results for hectorite show that the amount of intercalated CO_2 increases stepwise with increasing basal spacing, that with the alkali cations the amount increases with decreasing cation radius, and that for the alkaline earth cations the amount does not change significantly with cation radius (Figure 11, top panels). The computed potential energies show that with the relatively small cations in each series (Li^+, Na^+, Mg^{2+}, Ca^{2+}) the collapsed structure is the stable state. This result confirms the experimental observation that in the absence of H_2O to prop the interlayer open in montmorillonite, CO_2 does not enter it. With larger cations (K^+, Rb^+, Cs^+, Sr^+, Ba^+), the GCMD results show that the 1 or 2 layer hydrate states are stable relative to the collapsed state, consistent with the experimental results indicating expansion in these systems upon introduction of dry supercritical CO_2.

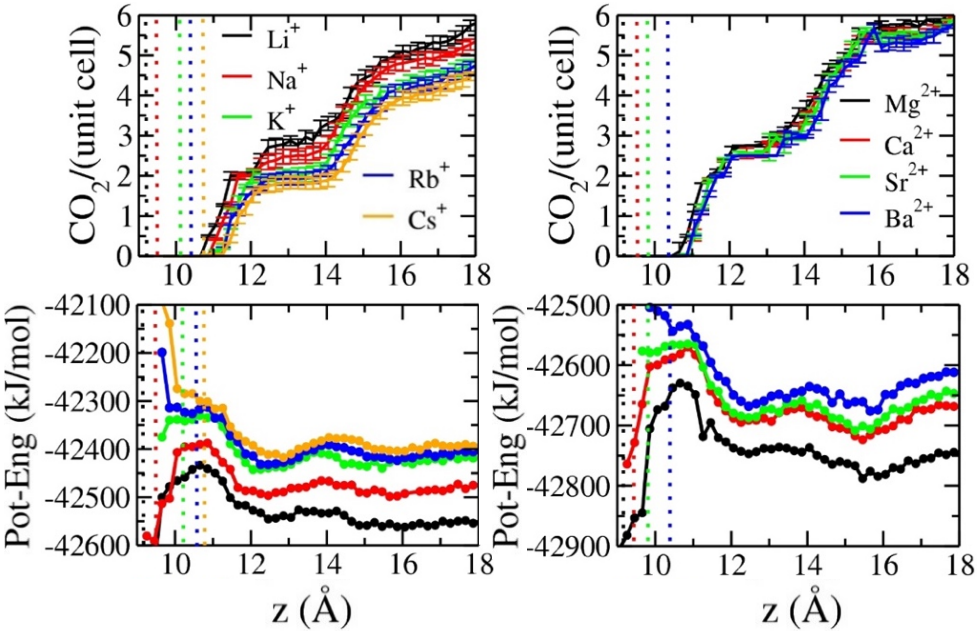

Figure 11. Number of intercalated CO_2 molecules (upper panels) and potential energies (lower panels) for hectorite with the indicated alkali and alkaline earth cations as functions of interlayer spacing obtained from GCMD simulations 323K and 90 bar CO_2 pressure with no H_2O in the systems. Dotted vertical lines indicate the collapsed interlayer spacing with the indicated cation.

The GCMD results also show that energetically this behavior is due principally to the decreasing difference in energy between the collapsed and solvated states with increasing cation radius due to decreasing cation-clay interactions (Figure 12). The decreasing energy of interaction between CO_2 and the cations with increasing cation radius is not sufficient to counteract this difference, and the energies of the clay-CO_2 interactions do not change significantly with the cation. The energetics of the CO_2-cation interactions reflect not just the fundamental solvation energies of the cations but also variation in the structural arrangements of the CO_2 around the cations imposed by the presence of the clay.

In parallel, our classical MD and adaptive-biasing-force modeling of Na-montmorillonite with a mixed mono-layer of 4 H_2O/Na^+ and 1.33 CO_2/Na^+ at 323K and 89 bars (paper 26, Table 1) shows that H_2O and CO_2 form a single layer in the middle of the interlayer, that the H_2O clusters around the Na^+, and that CO_2 is concentrated between these clusters. This configuration provides dynamic percolation pathways that allow single-file diffusion of the CO_2 molecules parallel to the clay layers and Na^+ diffusion between the two basal surfaces on either side of the interlayer.

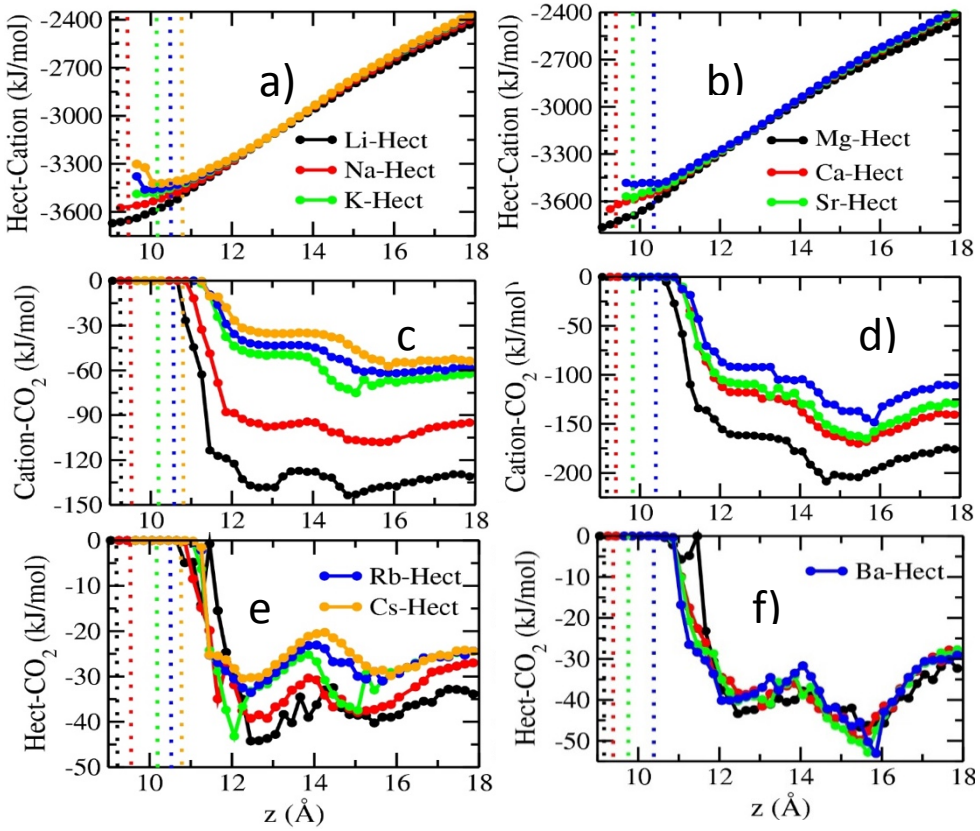

Figure 12. Computed variation in clay-cation, cation–CO_2, and clay-CO_2 interaction energies as functions of interlayer spacing for hectorite with the indicated alkali and alkaline earth cations at 323K and 90 bar in the systems with no H_2O described in Figure 11. Dotted vertical lines indicate the collapsed interlayer spacing with the indicated cation.

Similar classical MD modeling of Na-montmorillonite interlayers containing CO_2, poly(ethylene glycol) (PEG), and both CO_2 and PEG (paper 17, Table 1) provide a detailed structural model for the arrangement of this important model polymer in smectite interlayers and show that the arrangement of the CO_2 molecules is similar to that in supercritical CO_2. One of the important insights from this study is that the dry ice structure is a good reference model for CO_2 in systems containing O-atoms in the same way that the ice-1h structure is a reference model for the structure of liquid water. The results show that relative to the base clay, the cooperative motion of the Na^+ and CO_2 increases the Na^+ diffusion rate and demonstrate the importance of the –C-O-C- ether oxygens in coordinating to CO_2 molecules.

E. Clay-NOM-scCO$_2$ Interactions

Bowers et al. (paper 20, Table 1) describe the first *in situ* NMR experiments for clay-NOM-scCO$_2$ systems at conditions relevant to shale-gas extraction or geological CO$_2$ sequestration reservoirs (Na-hectorite ± Suwannee River HA; T = 323 K, P_{CO2} = 90 bar). The ^{13}C NMR spectra contain peaks for only ^{13}C-enriched CO$_2$ rapidly tumbling in the supercritical fluid phase but do show small line-width increases reflecting increased association of CO$_2$ with the base clay and clay-HA composite surfaces. The ^{13}C and ^{23}Na T_1 relaxation rates and the ^{23}Na line shapes show that CO$_2$ influences the Na^+ coordination environment and dynamics, leading to more symmetric Na^+ coordination and generally more rapid Na^+ relaxation with scCO$_2$ present. This is probably the result of removal of interlayer water due to its dissolution in the initially dry scCO$_2$. The presence of Suwannee River HA has little effect on the ^{23}Na or ^{13}C NMR spectra but does lead to slower T_1 relaxation rates for a portion of the ^{23}Na population with and without scCO$_2$ present.

F. Clay-scCH$_4$ Interactions

The interaction of mineral surfaces and interlayers with hydrocarbons is also critical to understanding the behavior of traditional and hydro-fracked petroleum and natural gas reservoirs as well as to the design and evaluation of alternatives to water-based fracking fluids (such as scCO$_2$-based gas extraction strategies). *In situ* ^{13}CH$_4$ MAS NMR, XRD, and IR experiments with hectorite at 323 K and 90 bars CH$_4$ pressure have provided significant new insight that highlight the potential impact of the proposed work (paper 34, Table 1). These data provide the first spectroscopic evidence of CH$_4$ adsorption in smectite interlayers under reservoir conditions, the first assignments of the NMR resonances for different CH$_4$ adsorption sites in clays, and the first detailed insight into the mechanisms of supercritical CH$_4$ adsorption by clays and how they relate to the fluid R.H. and the properties of the charge-balancing cation. The hectorites used in this study contain a range of exchangeable cations with different hydration energies, radii, and polarizability (Cs^+, Na^+, Ca^{2+}, Pb^{2+}). All samples were initially vacuum dried at 323 K before being exposed to variably wet scCH$_4$ in the IR or XRD instrument. The NMR samples received the same type of vacuum heating ("dry" samples) or were equilibrated at room temperature and pressure at 43% or 100% R.H before being exposed to dry scCH$_4$.

The ^{13}C MAS NMR results show that CH$_4$ can adsorb on external basal surfaces and in the interlayer galleries of the clays, as well as occurring in the bulk supercritical fluid (Figure 13). The occupancy of each environment depends on the relative humidity (RH) of the CH$_4$-rich fluid and the hydration energy and size of the charge-balancing cation. As RH increases, the fraction of interlayer and inter-particle CH$_4$ decreases, although with Cs^+ increasing H$_2$O initially increases CH$_4$ uptake due to an increasing number of potential sorption sites. Maximum interlayer CH$_4$ adsorption occurs when the mean basal spacing just permits methane intercalation (~11.5 Å), and interlayer sorption never occurs below this basal spacing. Sorption is greater with divalent cations than with monovalent cations (Figure 14). The amount of interlayer adsorption is greatest at low H$_2$O contents when there are many interlayer adsorption sites unoccupied by cations or H$_2$O and when the number of charge-balancing cations in the interlayer is relatively low. The results show that the ^{13}CH$_4$ NMR chemical shift is sensitive to the size of the cavity occupied by the molecules, giving rise to the differences in chemical shifts for interlayer CH $_4$ with different cations and at different hydration states. The resonance for the CH$_4$ in interparticle pores becomes more like that

of bulk scCH4 with increasing RH, reflecting less interaction with the clay surface. The *in situ* ATR-IR spectra show that adsorption of CH_4 reduces its tetrahedral, T_d, symmetry, giving rise to the forbidden ν_1 band for clay-associated CH_4. The *in situ* XRD data are fully consistent with the NMR and IR data. Taken together, the results indicate that CH_4 adsorbs to smectite interlayers principally by a weak hydrophobic mechanism dominated by dispersion-type forces, leading to a passive, space-filling model for its intercalation.

Our ongoing GCMD calculations show that entry of CH_4 into the interlayer of Na-smectites is energetically very unfavorable, but that with larger cations such as NH_4^+ and Cs^+ its interlayer sorption is essentially energy neutral (Figure 15). These results support the passive, space filling mode for interlayer CH_4 exchange, such as occurs when the basal spacing is expanded to >11.5Å by, a partial layer of water molecules.

The incorporation of CH_4 into smectite interlayers under low RH conditions may have important implications for fracking using supercritical CO_2, where the dry $scCO_2$ flood may dehydrate the interlayers and lead to CH_4 intercalation by smectite-like layers in shale. Further studies of $CH_4/CO_2/H_2O$ competition for adsorption sites are critical to explore this possibility and the fundamental chemical controls of the competitive behavior. Such studies are an important component of our proposed work over the upcoming three years.

The results suggest that under reservoir conditions smectite interlayers may provide a reservoir for CH_4 under low-water conditions.

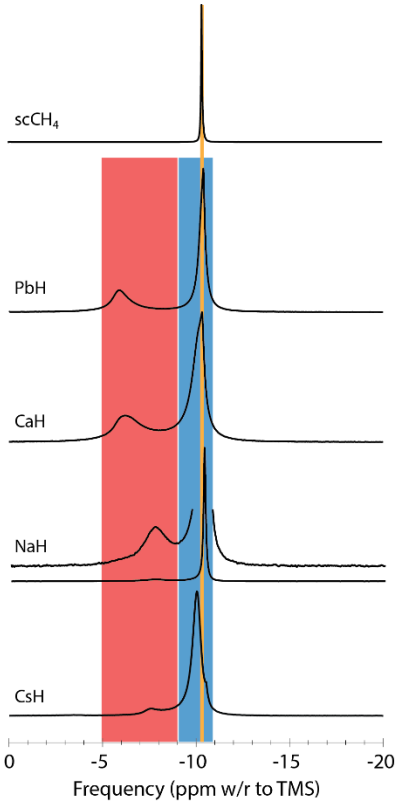

Figure 14. ^1H decoupled ^{13}C MAS NMR spectra of dry, isotopically enriched supercritical $^{13}CH_4$ with hectorite containing the indicated exchangeable cation. The samples we initially dried under vacuum at 50°C for 12-24 hours before being pressurized with $^{13}CH_4$ at 90 bar and 50°C. The red box marks the chemical shift region for the interlayer CH_4, the blue box CH_4 in external pores interacting with the clay surface(-10.2 ppm), and the orange line marks the position of bulk $scCH_4$. The peak for CH_4 in external pores is broadened due to the absence of complete isotropic averaging caused by association with the clay surfaces.

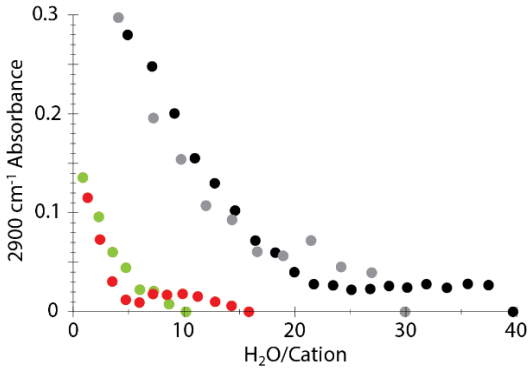

Figure 14. Intensity of the forbidden 2900 cm^{-1} $\square_1$ band for clay-associated CH_4 in the ATR-IR spectra versus the H_2O/cation determined from the transmission IR data for hectorite exchanged with the indicated cation. The color coding is: red = Na^+, green = Cs^+, grey = Pb^{2+}, and black = Ca^{2+}. The extent of CH_4 adsorption in much greater with the divalent cations, but in all cases the intensity of this band as the H_2O content increases, in agreement with the NMR results for these samples.

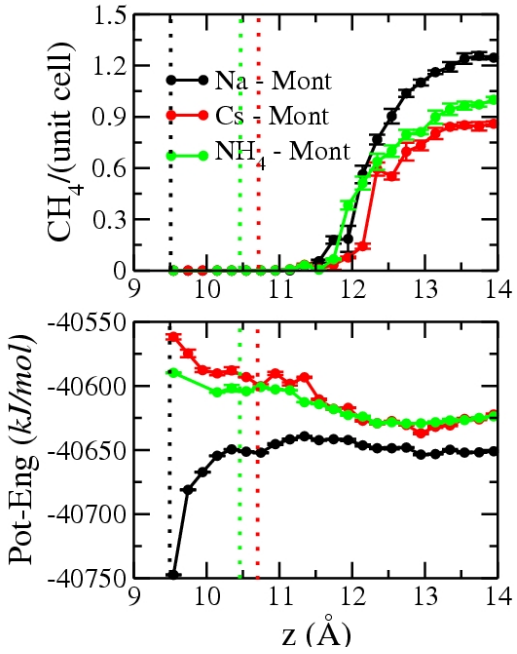

Figure 13. Interlayer CH_4 concentration in montmorillonite with the indicated exchangeable cation (top) and potential energy for CH_4 exchange into those interlayers (bottom) computed using GCMD calculations. The results support the interpretations of the experimental results that indicate that CH_4 enters the interlayers by a passive, space filling process driven by dispersive interactions.

III. Budget Explanation

There are no funds remaining in this grant.

IV. Estimate of Unobligated Balance

There is no unobligated balance for this grant.